



**HAL**  
open science

## Optimization strategy for the sizing of passive magnetic components

Guillaume Devos, Maya Hage-Hassan, Philippe Dessante, Cyrille Gautier,  
Adrien Mercier, Eric Labouré

► **To cite this version:**

Guillaume Devos, Maya Hage-Hassan, Philippe Dessante, Cyrille Gautier, Adrien Mercier, et al.. Optimization strategy for the sizing of passive magnetic components. 22nd European Conference on Power Electronics and Applications (EPE'20 ECCE Europe), Sep 2020, Lyon, France. pp.1-8, 10.23919/EPE20ECCEurope43536.2020.9215932 . hal-04548459

**HAL Id: hal-04548459**

**<https://hal.science/hal-04548459>**

Submitted on 16 Apr 2024

**HAL** is a multi-disciplinary open access archive for the deposit and dissemination of scientific research documents, whether they are published or not. The documents may come from teaching and research institutions in France or abroad, or from public or private research centers.

L'archive ouverte pluridisciplinaire **HAL**, est destinée au dépôt et à la diffusion de documents scientifiques de niveau recherche, publiés ou non, émanant des établissements d'enseignement et de recherche français ou étrangers, des laboratoires publics ou privés.

# Optimization strategy for the sizing of passive magnetic components

Guillaume Devos<sup>1,2</sup>, Maya Hage-Hassan<sup>1</sup>, Philippe Dessante<sup>1</sup>, Cyrille Gautier<sup>2</sup>, Adrien Mercier<sup>1</sup>, Éric Labouré<sup>1</sup>

<sup>1</sup>GEEPS – GROUP OF ELECTRICAL ENGINEERING, PARIS  
11, rue Joliot Curie  
Gif-sur-Yvette, France  
Tél: 01.69.85.16.33  
Fax: 01.69.41.83.18

<sup>2</sup>SAFRAN TECH  
1, Rue Jeunes Bois  
Châteaufort, France  
Tél: 01 61 31 80 00

E-Mail: guillaume.devos@centralesupelec.fr

## Keywords

Magnetic device, Airplane, Converter circuit, neural network, Device modeling, Energy converters for HEV, Passive component integration.

## Abstract

This paper presents an optimization methodology for the design of magnetic components embedded in aeronautical structures. We want to realize a multi-objective optimization of an inductance, taking into account some physical phenomenon that are not easily described with mathematical formulations, and to set up a methodology that allows us to harvest optimization time. We will use, for that purpose, analytical formulations, Finite Element Analysis (FEA), and a neural network to reduce the time consumption of components evaluation.

## Notations

$A_e$	$m^2$	core cross section
$\alpha$	-	Steinmetz parameter for frequency
$B_{max}$	T	maximum induction level
$\beta_F$	-	Steinmetz parameter for induction
$\Delta\theta$	K	Temperature elevation
$\eta$	-	efficiency
$f$	Hz	frequency
$h$	$W \cdot m^{-2} \cdot K^{-1}$	Heating coefficient
$J$	$A \cdot m^{-2}$	RMS current density
$k_w$	-	Winding coefficient
$k_i$	-	Mean current divided by RMS current
$K_{ripple}$	-	Current ripple divided by maximum of the current
$K_P$	-	Corrective Steinmetz parameter
$K_{P_t/P_c}$	-	Iron losses divided by copper losses
$K_S$	-	Exchange surface divided by $(A_e S_w)^{\frac{1}{2}}$
$k_v$	-	1 – duty cycle
$K_{V_c}$	-	Volume of copper divided by $(A_e S_w)^{\frac{3}{4}}$

$K_{V_i}$	-	Volume of iron divided by $(A_e S_w)^{\frac{3}{4}}$
$P_c$	W	Copper losses
$P_i$	W	Iron losses
$P_{max}$	W	Power flowing through the component
$R_{ac}/R_{dc}$	-	AC resistance divided by DC resistance
$\rho$	$\Omega.m$	Resistivity at given temperature
$S_w$	$m^2$	Winding path area
$N$	-	Winding number of turns

**Introduction**

The integration of more electrical power in the aerospace systems will help redefine the development of future aircrafts. Mass optimization of power converters based on Wide Band Gap semiconductors is essential for facing the challenges in the aerospace field brought about by the concepts of More Electrical Aircraft (MEA) and More Electrical Propulsion (MEP). In Fig. 1, a view to the exponentially increasing MEA and MEP development is presented [1].

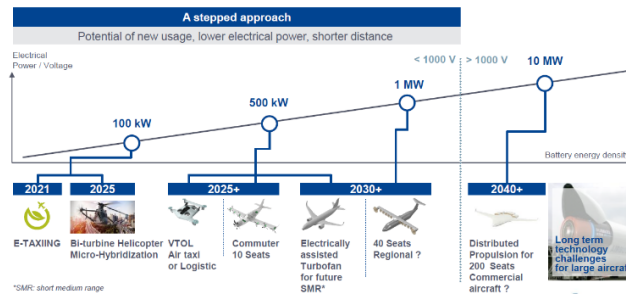


Fig. 1: a roadmap to hybrid electric energy & propulsion

In the field of More Electrical Propulsion, aircraft network architecture could include high-power propulsion electrical distribution network and storage equipment. In a configuration that includes a high voltage DC bus and a Li-ion battery, a non-isolated DC/DC converter can be inserted between the battery and the DC bus. The aim of this converter is to limit the voltage variations of the DC bus and to control the power flow of the battery. For a Li-ion battery of 540V, the voltage can vary from 400V to 630V depending on the state of charge. In the case of a DC bus voltage between 750V and 1000V, we choose to work on a multiphase synchronous boost converter, based on SiC transistors (fig. 2). In such a converter, weight optimization depends on the number of phases, the switching frequency and the magnetic components. To have an optimized sizing of the magnetic component according to the materials and other parameters is therefore most important. In addition, this optimization process must be fast enough to allow the evaluation of many converter configurations (frequency, number of phases, current ripple and magnetic material) and allow the computation of an overall optimum.

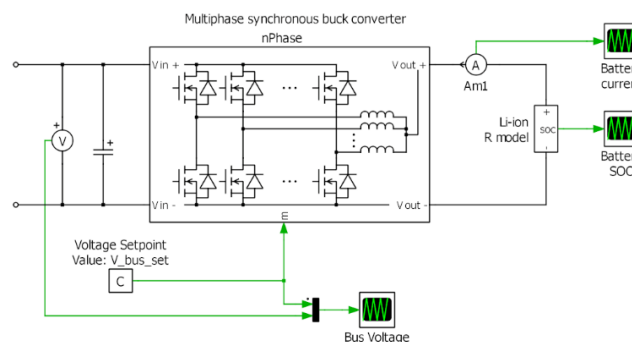


Fig. 2: Multiphase synchronous buck converter

This paper will present an optimization strategy. We used the design of a smoothing inductance located at the output of a DC/DC converter, carrying 1 kW at 25 kHz, as illustration of the global methodology. This strategy will take place in four stages:

1. A pre-sizing process with simplified analytical formulas (*coarse model*), gives a set of initial geometric and size solutions to the required specifications. We do not take into account AC losses in windings during this pre-sizing process.
2. Copper losses are refined on a few selected geometries using finite element software (FEMM 4.2 [2]) to calculate a  $R_{ac}/R_{dc}$  ratio taking into account eddy currents and proximity effects in the windings. This model based on finite element analysis is here after defined as fine model,
3. A surrogate model for copper losses is proposed, it is based on the correction of  $R_{ac}/R_{dc}$  ratio by means of a neural network model,
4. This substitute corrected model is then used in a stochastic multi-objective algorithm based on a “differential evolution algorithm” (DEA) [3].

## 1. Objective of the work

The general objective of this work is to optimize the previously described magnetic component. We want to minimize two variables:

- $$\left\{ \begin{array}{l} \text{- the weight} \\ \text{- the losses ratio (amount of losses divided by } P_{max} \text{, equal to } 1 - \eta) \end{array} \right.$$

Geometries are defined by 6 parameters:

- $$\left\{ \begin{array}{l} \text{- 4 geometric parameters (length and width of the winding path, width and depth of the magnetic central leg),} \\ \text{- the number of turns,} \\ \text{- the winding coefficient.} \end{array} \right.$$

The component is constrained by the saturation level of induction in the magnetic core.

The corresponding problem can be formulated as follow:

$$\min_x F(x) = \{Weight(x), 1 - \eta(x)\} \quad x = \{\ell_1, \ell_2, \ell_3, \ell_4, N, k_w\}$$

$$\text{Domain } \Omega : \left\{ \begin{array}{l} 0 < \ell_1 \leq L_{max} \\ 1 \leq N \leq N_{max} \\ 0 < k_{w_{min}} < k_w < k_{w_{max}} < 1 \end{array} \right.$$

Subject to  $g(x) \leq 0 : g(x) = B(x) - B_{max}$

## 2. Analytical pre-sizing process

The developments of our strategy are confined to the following design specifications:

- The designed magnetic component is a filter inductor designed for a Buck converter as represented in Fig. 3.a., carrying 1 kW at 25 kHz.
- The inductor voltage is +/- 135 V with an average current  $I_o$  of 7.4 A, a current ripple rate of 10% and a duty cycle of  $\frac{1}{2}$  (Fig. 3.b.).
- The magnetic core is a gapped ferrite core made with a 3C90 material. Its geometry is defined in Fig. 3.c.

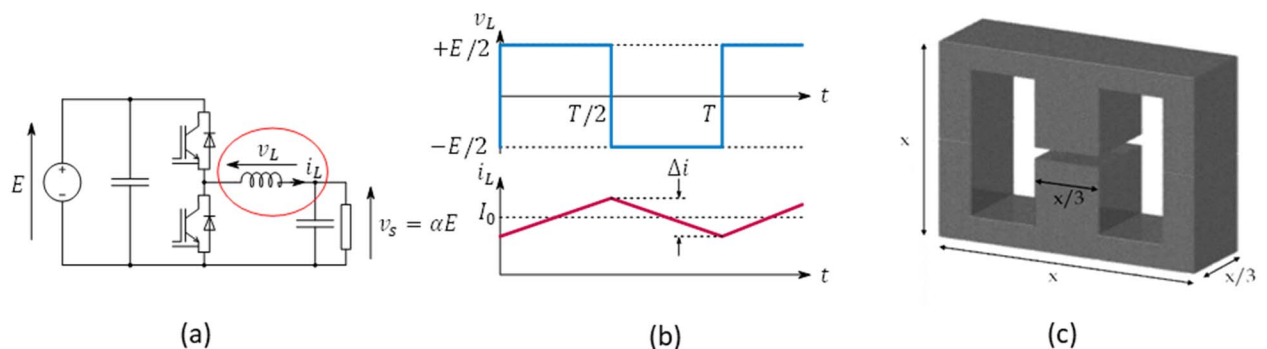


Fig. 3: a. schematic of the DC/DC converter. b. Current/voltage waveforms. c. Magnetic core shape.

Once the strategy is validated, it will be extended to others configurations. In the pre-sizing process, the geometry of all the components is assumed to be homothetic of a generic shape defined by the  $x$  parameter of Fig. 3.c.

The pre-sizing process is a mix between a thermally limited method [4] and a method using the area product “ $A_e S_w$ ” [5]. This method is based on the following formulation:

$$P_{max} \propto A_e S_w \times f \times J \times B_{max} \quad (1)$$

Many calculation models for core losses exist [6]. In this pre-sizing process, we have chosen a formula based on the Steinmetz equation, adapted for ferrites under this kind of electrical waveforms:

$$P_i = K_P f^\alpha (K_{ripple} \times B_{max})^{\beta_F} K_{V_i} (A_e S_w)^{\frac{3}{4}} \quad (2)$$

Electrical losses in windings are expressed by a formula that neglects AC component due to skin and proximity effects [7]:

$$P_c = \rho J^2 K_{V_c} (A_e S_w)^{\frac{3}{4}} \quad (3)$$

Considering a simple thermal model and introducing a ratio between iron and copper losses lead to the following formula for  $A_e S_w$  area product:

$$(A_e S_w)^{\frac{7\beta_F-2}{8\beta_F}} = \frac{k_v P_{max} (1 + K_{P_i/P_c})^{\frac{1}{\beta_F} + \frac{1}{2}}}{f k_i k_w} \times \frac{(K_P f^\alpha K_{V_i})^{\frac{1}{\beta_F}} (\rho K_{V_c})^{\frac{1}{2}}}{K_{P_i/P_c}^{\frac{1}{\beta_F}} (h K_S \Delta\theta)^{\frac{1}{\beta_F} + \frac{1}{2}}} \quad (4)$$

The calculation of the derivative with respect to  $K_{P_i/P_c}$  of this expression allows us to find that the volume of the component, when  $K_{P_i/P_c}$  increases, is decreasing then increasing. The minimum volume is reached for  $K_{P_i/P_c}$  equal to  $\frac{2}{\beta_F}$ .

However, this value of  $K_{P_i/P_c}$  can lead to a maximum induction level higher than the saturation level of the magnetic material. In this case, during the execution of the proposed algorithm, the value of  $K_{P_i/P_c}$  is decreased by steps of 10% while the saturation level is exceeded. A set of pre-sized components is computed using the implementation of this procedure (fig 4.a.) with different values for the temperature elevation ( $\Delta\theta$ ). The circles on Fig. 4.b represents the Pareto front of pre-sized components according to the previous inductor specifications and for temperature elevation in the range of 1 to 80 °C.

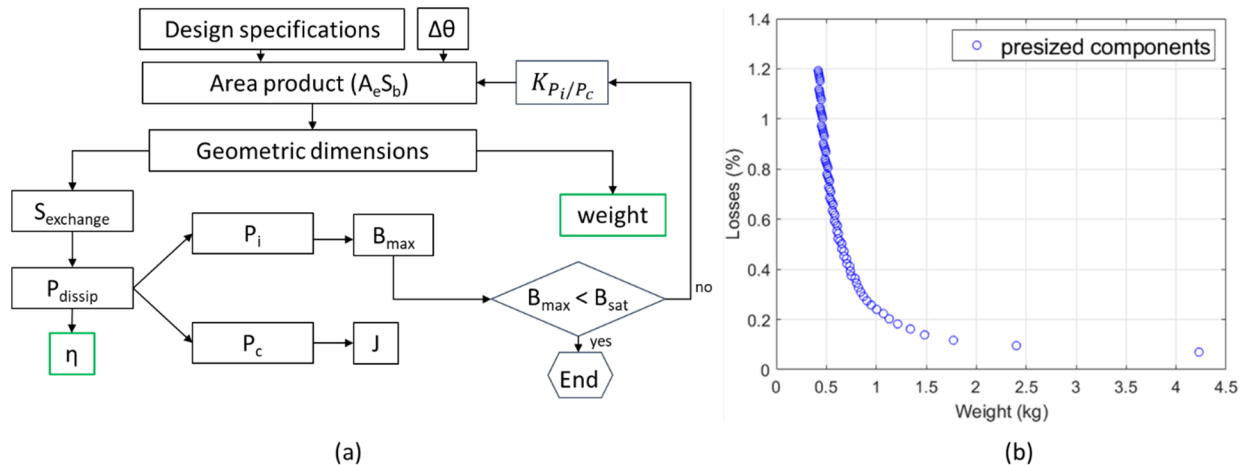


Fig. 4. (a) Flow chart of the pre-sizing process. (b) Pareto front of computed results ( $\Delta\theta$  between 1 and 80 °C).

The results of this analytical pre-sizing process is fed to a multiobjective DEA to find the Pareto based on this model. This analytical pre-sizing process gives a set of solutions based on the homothetic shape hypothesis presented in Fig.3. Computing a DEA with analytical formulations allows to quickly obtain a set of solutions for different geometric shape ratios.

### 3. Finite Element Analysis

The Analytical pre-sizing process doesn't consider eddy currents and proximity effects, a 2D Finite Element Method Analysis (FEA) is used to remedy this issue with the free software FEMM 4.2. Modeling a magnetic

component with detailed windings is time consuming, to overcome this issue, a homogenized model of the windings [8] has been used. The implementation of the homogenized model for windings drastically reduces the time required to calculate losses for a given component, from several minutes to a few seconds on a desktop computing station. In the context of our work, we use a laptop with a four-core CPU Intel core i5 7440 HQ (2.8 GHz). Considering a component with 64 turns (presented on Fig.5.), the calculation of  $R_{ac}/R_{dc}$  with detailed windings takes 6300 seconds whereas it takes only 16.6 seconds with the homogenized model.

The detailed and homogenized models have been compared on a frequency range between 100 Hz and 1 MHz in the fig 5.a. Calculations of  $R_{ac}/R_{dc}$  with homogenized model is close to the values obtained with detailed windings. The relative error between the two models does not exceed 3 %. This is quite acceptable while the calculation time is, according to previously given values, divided by approximately 400.

At this time, the effect of the gap on the center leg on  $R_{ac}$  losses is not taken into account. This will be done in future work, however, this does not fundamentally change the method.

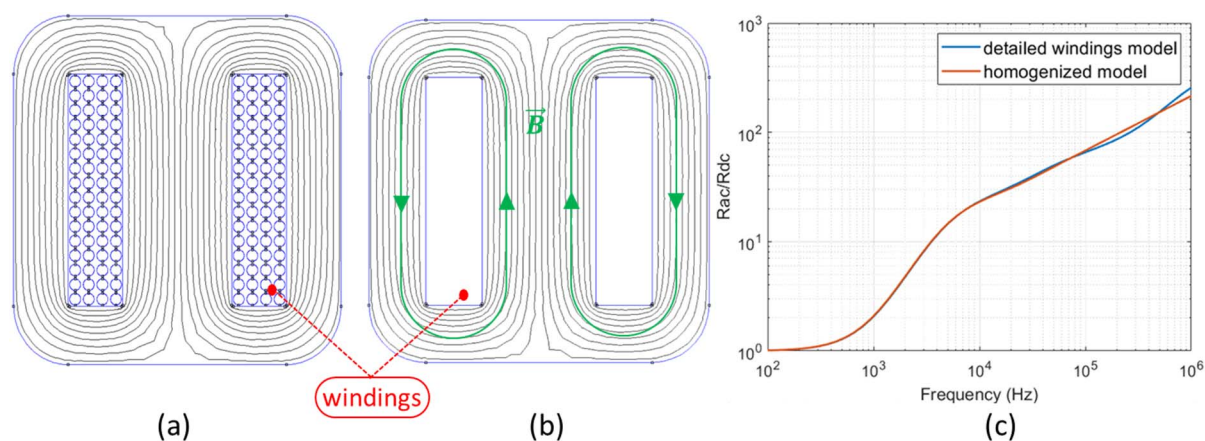


Fig. 5. (a) Detailed windings. (b) Homogenized model. (c)  $R_{ac}/R_{dc}$  as a function of frequency.

#### 4. Corrected copper losses model using a neural network

Although the implementation of the homogenized model for windings drastically reduces the time required to calculate losses for a given component (between several minutes and a few seconds), the gain in computation time does not allow for the systematic use of finite element analysis in an optimizing routine. For example, considering 15 seconds for one calculation in a procedure of 100 iterations with a set of 500 different geometries leads to approximately 208 hours exclusively dedicated to these analyses. As these results should be used in a more complex optimization process for the whole converter, it is therefore necessary to reduce the number of FEA evaluations, and then find a way to assign a  $R_{ac}/R_{dc}$  value for each geometry of the design space.

A methodology based on the Space Mapping Technique [9] is proposed and is described in Fig 6.a. The geometries were chosen with regular spacing on the Pareto front resulting from the optimization of the analytical pre-sizing model (fig 4b).

With this set of 124 geometries and their calculation via FEA, we construct an approximation of these data based on a neural network (using *newrb* function in Matlab software). Of this 124 geometries, 20 are used to train the neural network, and 104 are used for its validation.

Values of  $R_{ac}/R_{dc}$  has been calculated with FEMM for all these 124 points. In Fig 6.b we represent the value of  $R_{ac}/R_{dc}$  obtained by FEM calculation, and the approximation of  $R_{ac}/R_{dc}$  ratio that the neural network assigns to all the 124 points.

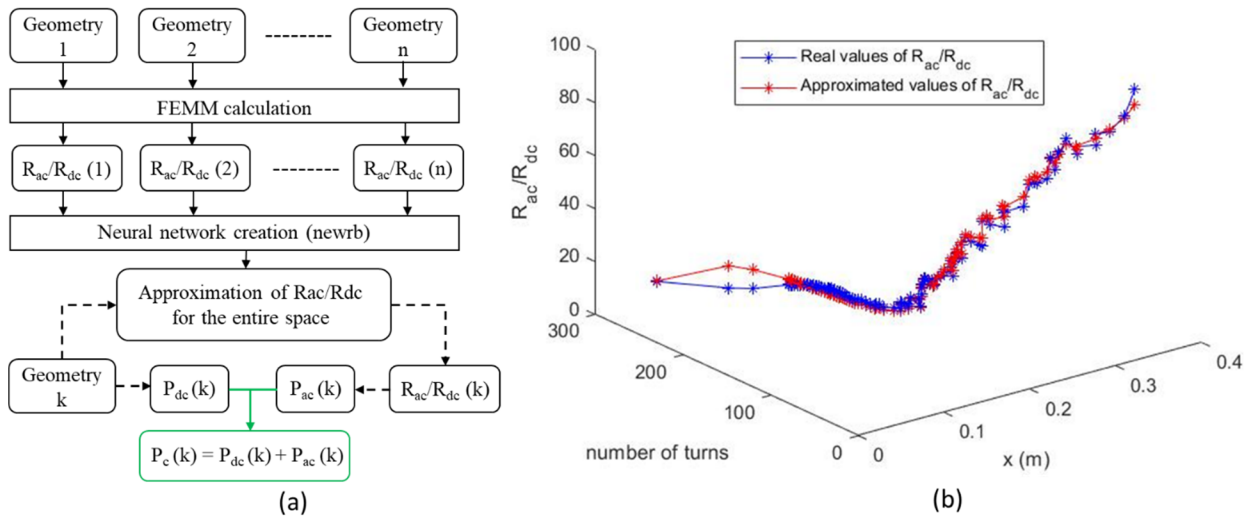


Fig. 6. (a) Space mapping: Flow chart of the creation and utilization of the neural network. (b) Construction of a neural network. In blue: FEM computed values of  $R_{ac}/R_{dc}$ . In red: approximated values of  $R_{ac}/R_{dc}$ .

This neural network gives a quite good approximation of  $R_{ac}/R_{dc}$ . We will use it in our optimization algorithm, and then verify its efficiency in this process.

**5. Global optimization strategy**

The adopted global strategy employed here is described by the flow chart in Fig.7.

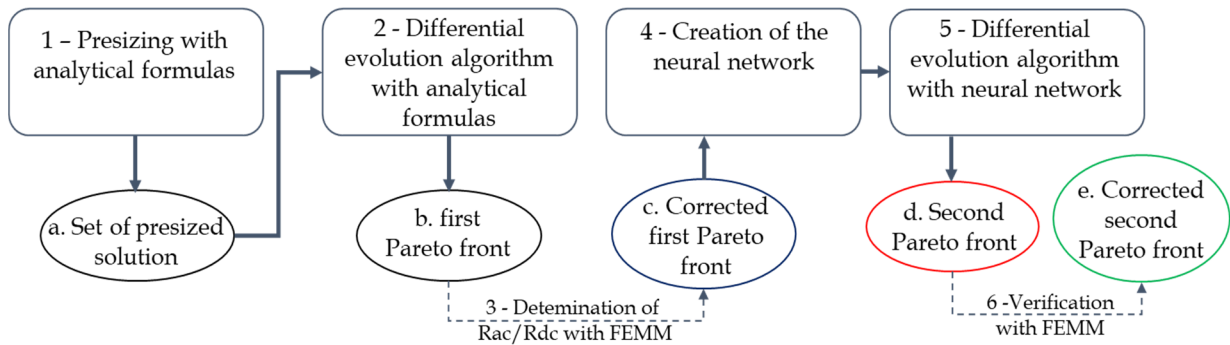


Fig. 7. Flow chart of the complete optimization strategy.

A first set of optimal geometries (Fig7.a) is computed using the analytical pre-sizing process (step 1 of fig.7, see also fig 4.). This set is fed to a first DEA (step 2) to compute a first optimal Pareto front (b). To take into account the AC effect in windings, we compute the FEA calculation of  $R_{ac}/R_{dc}$  of these geometries (step 3), and use the results (c) to train a neural network (step 4). This neural network approximation is used in a second DEA (step 5) to compute the second Pareto front (d). The final result (e) is then determined by a complete FEA of the results (step 6).

We represent the corrected first Pareto front (c, blue line), the one obtained after the second computation of DEA (d, red line) and its verification through FEMM (e, green line) on Fig.8.

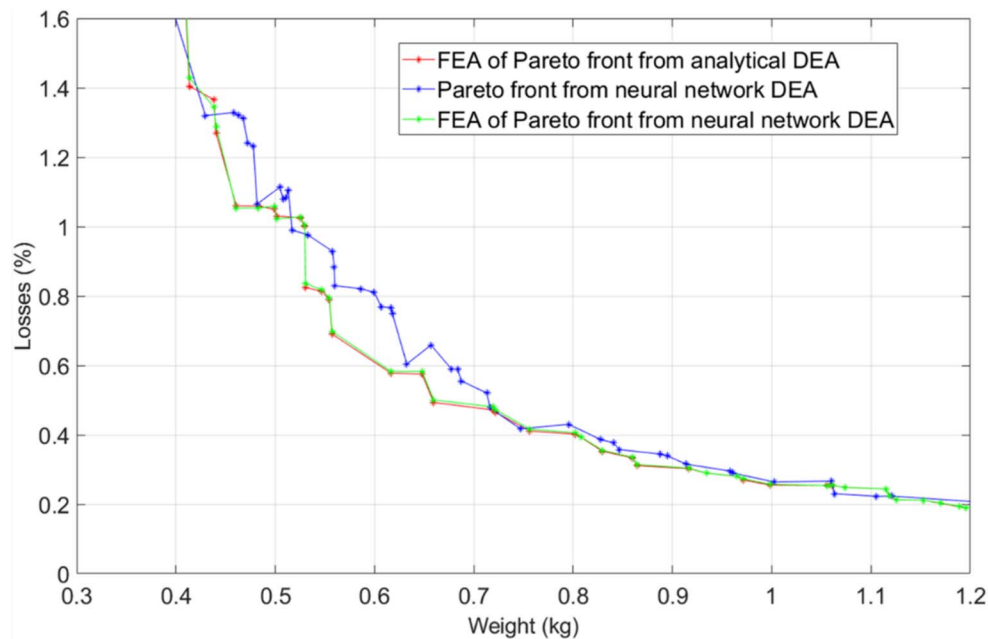


Fig. 8. Pareto optimal solutions obtained with analytical formulas and with neural network assignment

In order to verify the accuracy of the neural network and the need to consider AC effects during the optimization process, we represent three sets of solutions.

Indeed, the comparison between the Pareto front obtained after the second DEA (red line), and its correction with FEA analysis (green line) shows little differences between these two sets. It allows us to admit the good accuracy of the neural network in the attribution of  $R_{ac}/R_{dc}$  for these geometries.

The comparison between the Pareto front obtained after the first DEA, corrected by FEA (blue line) and the FEA correction of the second Pareto front (green line), shows that the geometries obtained after the second DEA present lower level of losses for a same weight, than those obtained without consideration of AC effects during DEA. We can conclude that it is important to take into account AC effects during the DEA in order to reach better optimized solutions.

## Conclusion

The proposed optimization methodology provides an efficient way to design components in which physical phenomena cannot be estimated correctly with analytical models. The proposed solution uses few Finite Element calculations and a neural network to extend these calculations to the entire design space. In further works, we will apply this methodology to other specifications and at different frequencies. We will also try to adapt this methodology in order to consider the presence of an air gap on the electrical losses of the component.

## References

- [1] V. Garnier, Perspectives and activities on hybrid / electric propulsion, MEA 2019, Toulouse
- [2] Crozier, R, Mueller, M., "A New MATLAB and Octave Interface to a Popular Magnetics Finite Element Code", Proceedings of the 22nd International Conference on Electric Machines (ICEM 2016), September 2016
- [3] Storn, Rainer & Price, Kenneth. (1997). Differential Evolution - A Simple and Efficient Heuristic for Global Optimization over Continuous Spaces. *Journal of Global Optimization*. 11. 341-359. 10.1023/A:1008202821328.
- [4] A. Van den Bossche et V. Cekov Valchev, « Inductors and Transformers for Power Electronics ». CRC Press, 2005.
- [5] F. Forest, E. Laboure, T. Meynard and M. Arab, "Analytic Design Method Based on Homothetic Shape of Magnetic Cores for High-Frequency Transformers," in *IEEE Transactions on Power Electronics*, vol. 22, no. 5, pp. 2070-2080, Sept. 2007.
- [6] Krings, Andreas & Soulard, Juliette. (2010). Overview and Comparison of Iron Loss Models for Electrical Machines. *Journal of Electrical Engineering*. 10. 162-169.



- [7] C. R. Sullivan, "Computationally efficient winding loss calculation with multiple windings, arbitrary waveforms, and two-dimensional or three-dimensional field geometry," in *IEEE Transactions on Power Electronics*, vol. 16, no. 1, pp. 142-150, Jan. 2001.
- [8] D. C. Meeker, "An improved continuum skin and proximity effect model for hexagonally packed wires", *Journal of Computational and Applied Mathematics*, Volume 236, Issue 18, 2012, Pages 4635-4644.
- [9] Hage Hassan, M., Remy, G., Krebs, G. and Marchand, C. (2014), "Radial output space mapping for electromechanical systems design", *COMPEL - The international journal for computation and mathematics in electrical and electronic engineering*, Vol. 33 No. 3, pp. 965-975.
- [10] MATLAB and deep learning Toolbox 2018b, The MathWorks, Inc., Natick, Massachusetts, United States.